Phase Partition Analysis of Nucleotide Binding to Axonemal Dynein†

Gabor Mocz* and I. R. Gibbons

Pacific Biomedical Research Center, University of Hawaii, Honolulu, Hawaii 96822

Received March 18, 1996; Revised Manuscript Received May 6, 1996⊗

ABSTRACT: The binding of nucleoside triphosphates and related ligands to dynein ATPase from sea urchin sperm flagella has been studied by equilibrium partition analysis in an aqueous biphasic system containing dextran and poly(ethylene glycol). The stoichiometry of binding and the corresponding stepwise binding constants are obtained from direct binding isotherms fitted to the primary data. The results suggest that dynein possesses four different binding sites for nucleoside triphosphates per mole of heavy chain. The stepwise binding constants for MgATP range from $\sim 10^4$ M^{-1} to $\sim 10^5$ M^{-1}. The isolated α and β heavy chains have binding parameters similar to intact dynein. The amount of ADP bound normally is ∼75% that of ATP, both for the intact dynein and for the separated heavy chains, although full saturation is achieved at high nucleotide concentrations. In the presence of the ATPase inhibitor vanadate, ADP binds with affinities similar to those of ATP, with binding constants close to those of ATP in the absence of vanadate. No appreciable binding of AMP or EDTA/ATP is observed. The substitution of Ca^{2+} or Fe^{3+} for Mg^{2+} does not significantly alter the amount of ATP bound; however, CaATP is bound with a somewhat lower affinity. Scatchard and Hill plots of the binding data and the calculated site-binding constants suggest that ATP and ADP bind in a weakly cooperative manner. These results suggest that the multiple binding of nucleotide to dynein heavy chains occurs at physiological concentrations, putatively at the four binding sites predicted earlier on the basis of their amino acid sequences. The data are consistent with a model in which, in addition to a single catalytic site, nucleotide binding occurs at additional noncatalytic sites that represent an as yet unknown functional aspect of dynein.

Dynein ATPase is a high molecular weight energy-transducing motor protein involved in many forms of microtubule-based cell motility including ciliary and flagellar movement, chromosome movement, and organelle and vesicle transport. Two major classes of dynein, axonemal (Gibbons 1963, 1989) and cytoplasmic (Pallini et al., 1983; Paschal et al., 1987), have been described so far. Axonemal dyneins are responsible for the generation of sliding between tubules that produces the motility of cilia and flagella (Gibbons, 1981). Cytoplasmic dynein is present in both ciliated and nonciliated cells (Pallini et al., 1983; Lye et al., 1987; Neely et al., 1990) and is involved in organelle and vesicle transport toward the minus end of cytoplasmic microtubules (Vallee et al., 1989; Schnapp & Reese, 1989) and in a wide variety of essential cellular movements (Asai & Lee, 1995).

All dyneins are proteins of 1200−1900 kDa that contain characteristically very large subunits of 500 kDa (α, β, and γ in homo- or heterooligomer combinations) as well as several intermediate chains of 75−150 kDa and light chains of 15−25 kDa. The β heavy chain of axonemal dynein, which retains the capability for microtubule translocation *in vitro* (Sale & Fox, 1988; Vale et al., 1989), has been central to the study of dynein function. Axonemal dyneins are highly specific for ATP as substrate (Gibbons, 1966; Ogawa & Mohri, 1972). Other nucleoside triphosphates are hydrolyzed at substantially lower rates, and they usually do not support axonemal movement (Shimizu et al., 1991). In cytoplasmic dyneins, CTP is more rapidly hydrolyzed *in vitro* than ATP, but only ATP supports microtubule gliding *in vitro* (Pallini et al., 1982; Hays et al., 1994).

Heavy chain sequences have recently been obtained by molecular cloning both for axonemal (Gibbons et al., 1991; Ogawa, 1991; Wilkerson et al., 1994; Mitchell & Chang, 1994) and cytoplasmic dyneins (Koonce et al., 1992; Mikami et al., 1993). A characteristic feature in all the deduced sequences is the occurrence of the sequence fingerprint for a nucleotide-binding site, P-loop (Walker et al., 1982), at four locations spaced about 300 residues apart in the midregion of the heavy chain. The P-loop corresponding to the probable hydrolytic ATP-binding site, P1, can be identified by its location close to or at the V1 site of vanadate-mediated photocleavage and is the P-loop closest to the N-terminus (Gibbons & Mocz, 1990). Since dynein ATPase activity decreases in direct proportion to the fraction of photocleavage at this site (Gibbons et al., 1987), it is unlikely that any of the other putative binding sites hydrolyzes ATP at an appreciable rate. Kinetic analysis of the ATPase activity of *Tetrahymena* dynein shows simple Michaelis−Menten kinetics with a K_m of about 1 μM (Johnson, 1983). The region around the hydrolytic site, P1, has the most highly conserved sequence among dynein isoforms (Koonce et al., 1992; Mikami et al., 1993; Gibbons et al., 1994). The less tightly conserved sites, P2−P4, may constitute parts of regulatory nucleotide-binding sites that represent an as yet unknown functional aspect of the dynein heavy chain.

Within the last few years, new data for multiple, functionally distinct nucleotide binding sites on dynein have surfaced.

† This work was supported by National Institute of Health (NIH) Grant GM-30401.

* Address correspondence to this author at Kewalo Marine Laboratory, 41 Ahui St., Honolulu, HI 96813. Phone: (808) 539-7326. Fax: (808) 599-4817. E-mail: gmocz@hawaii.edu.

⊗ Abstract published in *Advance ACS Abstracts,* June 15, 1996.

S0006-2960(96)00662-9 CCC: $12.00

In particular, the sliding disintegration of *Tetrahymena* cilia and *in vitro* motion of *Chlamydomonas* axonemes are inhibited by high concentrations of ATP, and this inhibition can be reversed by addition of ADP (Kinoshita et al., 1995; Wilkerson & Witman, 1995). Similarly, a high concentration of ATP inhibits the flagellar movement of *Chlamydomonas* pf mutants, and ADP antagonizes this inhibition (Omoto et al., 1996). Both *Chlamydomonas* dynein and its γ heavy chain subfraction show nonlinear kinetics of ATP hydrolysis at submillimolar ATP with two K_m's of 8−11 and 66−80 μM, respectively, indicating that each dynein heavy chain has at least two functional ATP binding sites, one high-affinity binding site, and at least one lower affinity nucleotide-regulatory site (Wilkerson & Witman, 1995).

In order to obtain more detailed information on the number and properties of the binding sites, we have examined the binding reaction under equilibrium conditions. Partition equilibrium in an aqueous biphasic dextran−poly(ethylene glycol) polymer system permits a rapid equilibration of nucleotide between the phases that has allowed us to measure directly the equilibrium binding of both hydrolyzable and nonhydrolyzable nucleotides. This method has been used previously in studies of nucleotide binding to aspartate transcarbamylase (Gray & Chamberlin, 1971) and formyltetrahydrofolate synthase (Curthoys & Rabinowitz, 1971) as well as in the study of a variety of simple and macromolecular binding reactions (Albertson, 1983). In the present study, this approach has been used to monitor the binding of the physiologically important adenine nucleotides to axonemal dynein and its heavy chain subfractions from sea urchin sperm flagella. The present results, which are the first direct measurements of equilibrium binding of nucleotides to dynein, suggest that each dynein heavy chain contains four different nonequivalent binding sites that may have cooperativity. A preliminary report of this work has been presented (Mocz & Gibbons, 1995).

MATERIAL AND METHODS

Chemicals. Dextran (average M_w 580 000) and polyethylene glycol (average M_w 8000) were obtained from Sigma (St. Louis, MO). The polymer solutions used in the partition equilibrium experiments were prepared by dissolving these compounds in 100 mM K_2SO_4 and 25 mM Tris/H_2SO_4, pH 7.4. Adenine nucleotides (ATP, ADP, AMP, AMPPNP) came from Boehringer Mannheim (Germany) and were shown by phosphate assay (LeBel et al., 1978) to contain <5% of hydrolyzed nucleotides. Nucleotide concentrations were determined spectrophotometrically (A_{259} = 15 400). Iron gluconate was synthesized as described earlier (Mocz & Gibbons, 1990). All other chemicals were analytical grade from Sigma (St. Louis, MO).

Protein Preparations. Outer arm dynein with latent ATPase activity was extracted from sperm of the sea urchin *Tripneustes gratilla* as described previously (Bell et al., 1982). The dynein was then transferred to 0.5 M acetate-based medium by dialysis and purified to remove tubulin by centrifugation on sucrose density gradients. The separated α and β heavy chain fractions were obtained by dialysis of the dynein against a 1 mM EDTA and 25 mM Tris/H_2SO_4, pH 7.4 medium, followed by centrifugation on 5−20% sucrose gradients (Bell et al., 1982). All samples were concentrated by precipitation with 60% saturated $(NH_4)_2SO_4$ and then dialyzed into a medium containing 100 mM K_2SO_4 and 25 mM Tris/H_2SO_4, pH 7.4 before beginning partition equilibrium experiments.

Equilibrium Partition. Binding of adenine nucleotides to dynein and its heavy chain fractions was determined by the method of partition equilibrium as developed by Gray and Chamberlin (1971). A scaled up version of the method was used to facilitate spectrophotometric determination of the unbound nucleotides. Stock solutions of poly(ethylene glycol), dextran, protein, ligand, and buffer were combined in a final system of 1.25 mL such that the final mean concentrations of dextran and poly(ethylene glycol) were 7.0 and 7.5%, respectively. Samples were prepared with a wide range of nucleotide to dynein ratio, always with the same constant amount of one component. The protein concentrations used were in the range 0.6−6 mg/ml in the dextran phase, and nucleotide concentrations in the same phase were 5−500 μM. For most experiments, the protein concentration was kept constant. All samples contained 100 mM K_2SO_4 and 25 mM Tris/H_2SO_4, pH 7.4. K_2SO_4 partitions almost equally between the two phases and so minimizes electrical potential differences at the phase interface. The samples also contained 2 mM $MgSO_4$, 1 mM $CaSO_4$, 0.5 mM Fe(III)-gluconate, 0.5 mM EDTA, or 50−100 μM vanadate, as required for a particular experiment. After combining the constituents, samples were thoroughly mixed on a vortex mixer and were allowed to incubate for 1 min before centrifugation to separate the phases. The phases were separated by centrifuging in an Eppendorf bench centrifuge for 5 min at 10 000 rpm. Subsequently, an aliquot was removed from the probe (upper) phase, and nucleotide concentration was determined spectrophotometrically (A_{259} = 15 400). Spectrophotometric blanks were obtained from identical phase systems lacking protein or nucleotide, as required. Since protein and ligand partition coefficients could shift somewhat as the ligand concentration was varied in a set of binding assays, the partition coefficients were redetermined at each protein and ligand concentration for each set of experiments. The volumes of the two phases were determined for several blank samples, and the average value was used in the calculations. All experiments were carried out at 23 °C. The nucleotide ligands were found to partition almost equally between the two phases.

Calculations. In the absence of protein we measure the equilibrium distribution of the nucleotide between the two phases. The equilibrium constant for this process is called the partition coefficient and can be written as

$$P_o = m_{oS2}/m_{oS1} \quad (1)$$

where m_{oS2} and m_{oS1} represent the total molar concentration of the nucleotide at equilibrium in the indicated phase: 1, dextran; 2, poly(ethylene glycol), the probe phase. When protein has been added to phase 1, the apparent partition coefficient is defined as

$$P = m_{tS2}/m_{tS1} \quad (2)$$

where m_{tS2} and m_{tS1} are the total molar concentrations of the nucleotide in the two phases. The concentration m_{tS2} in phase 2 is measured, and the concentration m_{tS1} is then calculated by difference. Suppose the nucleotide is initially present, at concentration m_{iS1}, only in phase 1. At equilib-

rium the concentration in phase *2* is m_{tS2}. The total amount of nucleotide is therefore $m_{iS1}V_1$, and the amount in phase 2 is $m_{tS2}V_2$, where V_1 and V_2 are the volumes of phases 1 and 2. We therefore obtain

$$P = m_{tS2}/(m_{iS1} - Rm_{tS2}) \quad (3)$$

where $R = V_2/V_1$. Because only the free nucleotide partitions into phase 2, we have $m_{tS2} = m_{S2}$, where m_{S2} represents the free nucleotide in phase 2. The free nucleotide concentration m_{S1} in phase 1 is obtained by eq 1. Thus the experimentally determined apparent partition coefficient is a function of free ligand concentration in phase 1.

The extent of nucleotide binding, *r*, can be related to m_{S1}. The quantity *r*, interpreted as the average number of nucleotide molecules bound per dynein heavy chain, is calculated with

$$r = (m_{tS1} - m_{S1})/m_{tA1} \quad (4)$$

where m_{tS1} and m_{tA1} are the total concentration of the nucleotide and dynein, respectively, in the dextran phase. Therefore the experiment yields *r* as a function of m_{S1}. This was analyzed by fitting of the binding isotherm to the primary data using a general multiple stepwise equilibrium model (Nichol & Winzor, 1981):

$$AS_{i-1} + S = AS_i; \qquad m_{ASi} = K_i m_{ASi-1} m_S; \quad (i = 1, 2, ..., p) \quad (5)$$

where K_i is the equilibrium binding constant on a molar scale and *p* is the maximum number of binding sites; *A*, dynein, *S*, nucleotide. From eq 4, *r* can be expressed as a function of K_i and m_{S1}:

$$r = \sum_i i(\prod_l K_l) m_{Si}/(1 + \sum_i (\prod_l K_l)) m_{Si}; \quad (i = 1, ..., p; l = 1, ...i) \quad (6)$$

This is a ratio of polynomials in m_S, valid for the dextran phase and independent of m_A and of the total dynein concentration.

Estimating the binding constants involves minimizing an error function, $E(r,\underline{r})$ where *r* is the measured experimental value and $\underline{r}$ is the calculated molar ratio of bound nucleotide to dynein after fitting the model. To recover the parameters, a simplex optimization procedure (Cooper, 1981)

$$E(r,\underline{r}) = \sum |r - \underline{r}| \quad (7)$$

was used with initial estimates of

$$K_i = (r - i + 1)/[(i - r)m_A] \quad (8)$$

An alternative method of obtaining estimates for the binding constants was also employed through the application of the widely used Levenberg−Marquardt nonlinear least-squares procedure (Press et al., 1992). Both methods agreed to the magnitude of the binding constants. However, the simplex method followed the experimental data more closely and was therefore the method of choice in this work.

To facilitate the interpretation of the calculated parameters, the stoichiometric constants, K_i, were transformed into site-binding constants, k_i, via the relation (Nichol & Winzor, 1979)

$$K_i = (p - i + 1)k_i/i \quad (9)$$

Computations used programs written in Turbo Pascal in this laboratory.

Reproducibility of Measurements. Within any single dynein preparation, measurements of the concentration of nucleotide in the probe phase agreed to 5−10% in duplicate samples. Estimates of error propagation for ligand binding indicated that values for *r* should be reliable to ±0.1−0.5 nucleotide bound per chain. Between different dynein preparations, the number of binding sites was consistently the same, but the calculated equilibrium binding constants showed larger variation.

Protein Concentrations. Protein concentrations were determined spectrophotometrically by an absolute method based upon the difference in absorbance at 235 and 280 nm (Whitaker & Granum, 1980). Alternatively, protein concentration was measured by the protein-independent method of Raghupathi and Diwan (1994). The two methods agreed within ∼5%. Molar subunit concentrations were calculated with values of 750 000, 650 000, and 550 000 for the intact dynein, the β heavy chain subunit, and the α heavy chain subunit, respectively.

Determination of ATPase Activity. ATPase activity of stock solutions of dynein and of dynein in the phase fractions was measured at room temperature in 100 mM K_2SO_4, 2 mM $MgSO_4$, and 25 mM Tris/H_2SO_4, pH 7.4. The inorganic phosphate liberated was determined by the method of LeBel (1978).

RESULTS

Characteristics of Dynein in the Dextran−Poly(Ethylene Glycol) Phase System. Analysis of the partition of protein between the dextran phase and the poly(ethylene glycol) phase by spectrophotometry at 280 nm showed that dynein and its heavy chain subfractions partitioned almost completely into the dextran phase at neutral pH and ionic strength below 0.2 M, presumably as a consequence of their high molecular weights. This distribution was confirmed by assay of dynein ATPase activity in the two phases, which showed that 96−98% of the Triton-activated ATPase activity partitioned into the dextran phase and less than 1% of it into the poly(ethylene glycol) phase, with a total recovery of 96−98% of the initial activity.

More detailed study of the effect of partition into the dextran phase on dynein ATPase activity showed that latent ATPase activity became 2−4-fold partially activated, which is 20−40% of the level of activation observed previously by exposing dynein to a variety of organic solvents (Evans & Gibbons, 1986). This partially elevated level could be further activated by Triton X-100 to the same level that was obtained by direct Triton X-100 activation of dynein that has not been subjected to partition. The activation of latent ATPase activity was reversible for exposures shorter than 20 min, and the activation became irreversible upon more prolonged exposures exceeding 1 h. These data indicate that, apart from partial loss of latency, the catalytic activity of dynein is little affected by exposure to the polymer phase system.

Preliminary experiments showed that binding of ATP to dynein reaches equilibrium within 1 min or less, and remains stable for 15−20 min at 23 °C. Thus measurements of

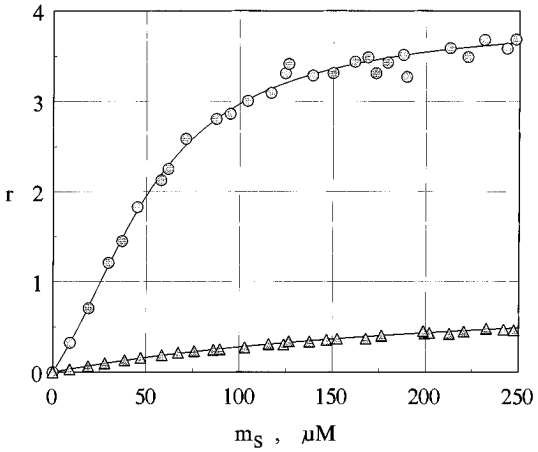

FIGURE 1: Binding of MgATP to dynein by equilibrium partition. Equilibrium partition experiments were carried out at 23 °C in the standard two phase system containing mean concentrations of 7.0% (w/w) dextran, 7.5% (w/w) poly(ethylene glycol), 0.1 M K_2SO_4, 25 mM Tris/SO_4, pH 7.4, 2 mM $MgSO_4$, and varying amounts of ATP. Intact dynein (circle) was present in the dextran phase at 5 μM; free MgATP concentration in the dextran phase ranged up to 250 μM. Data are shown as direct binding plot with r representing the moles of MgATP bound per mole of dynein heavy chain subunit (m_r 750 000) and m_S representing the concentration of unbound MgATP in the dextran phase. Binding of MgATP to free/oligomeric tubulin (triangle), separated from dynein on the same sucrose gradient, is also shown. Tubulin (m_r 55 000) concentration at equilibrium was 20 μM. The points in the figure are experimental, and the solid curve represents best-fit values. The data show a single representative experiment. Twenty-five separate experiments gave similar results within experimental error (see Table 1).

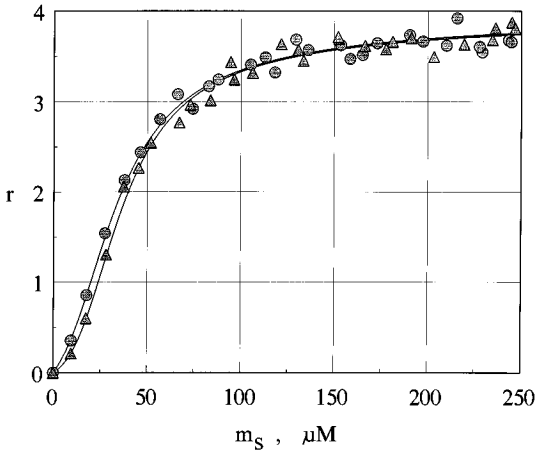

FIGURE 2: Binding of MgATP to α and β heavy chain subunits of dynein. The experimental conditions and abbreviations were as in Figure 1. (Circle) β heavy chain subunit (m_r 650 000); (triangle) α heavy chain subunit (m_r 550 000). The concentration of heavy chain subunit used for each binding curve was 4 μM in the dextran phase.

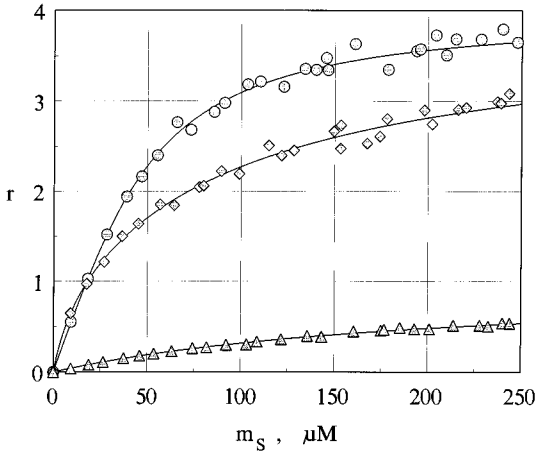

FIGURE 3: Binding of MgATP, MgADP, and MgAMP to the β heavy chain subunit of dynein. Conditions were as in Figure 1. (Circle) ATP; (square) ADP; (triangle) AMP. β heavy chain concentration in the dextran phase was 4 μM.

equilibrium binding of ATP were feasible without using a regenerating system, which would have greatly complicated the analysis.

Binding Curves with MgATP. Data from a typical equilibrium experiment measuring the binding of MgATP to intact dynein are shown in Figure 1. Binding of MgATP is expressed in terms of r, the mean number of moles of ATP bound per mole of dynein heavy chain as a function of m_S, the molar concentration of free ATP in the dextran phase. There are approximately three and a half binding sites per heavy chain. The curve indicates the presence of a relatively high affinity site at low values of m_S and of incipient saturation at an $r \sim 3.5$. The data could be fitted by assuming four distinct binding sites, and the solid line in Figure 1 is the reconstructed binding plot.

Since binding of ATP to polymeric tubulin is in the range 10^{-4} M (O'Brien & Erickson, 1989), we were concerned to exclude the possibility that a significant fraction of the nucleotide binding in our preparations of dynein might be due to traces of tubulin contamination. From a typical sucrose gradient purification, we pooled the fractions containing the tubulin which sediments more slowly (4−6S) than the fractions containing the dynein (18−20S). Assay of MgATP binding, however, showed that the tubulin fraction has only limited capability to bind MgATP, $r \sim 0.5$ at 250 μM free ATP (Figure 1). Since the amount of tubulin contaminating our purified dynein preparations was estimated as 2% by mass or 15% on a molar basis, it could not account for more than a few percent of the binding we observe.

Comparable data on MgATP binding for the separated α and β heavy chain fractions are given in Figure 2. Each of the separated heavy chain subunits binds MgATP to essentially the same extent as intact dynein. In some preparations, direct binding plots of the α heavy chain subunit, and to a smaller extent the β heavy chain subunit, showed some sigmoidicity at low levels ($r \sim 1$) of bound nucleotide where the error associated with the measurements is relatively large and reproducibility is lower. However, the maximum number of bound nucleotides was found to be the same in all preparations.

Binding of MgADP. Representative results for the interaction between the β heavy chain subunit and ATP, ADP, and AMP are shown in Figure 3. Although the overall trend of binding is similar for ATP and ADP, significant differences do occur. Except at low micromolar m_S, the binding of ADP appears to be weaker than that of ATP. At 250 μM m_S, the β heavy chain subunit binds approximately three ADP molecules. When similar measurements were done using higher concentrations of MgADP, ∼400−500 μM was required to attain the same level of binding as observed with ATP. Similar results were obtained with intact dynein.

In an experiment in which the incubation time with MgATP was extended from 1 min to 1 h prior to separation of the phases, in order to allow the ATP to become hydrolyzed by dynein to ADP, a binding isotherm similar to that of MgADP in Figure 3 was obtained as expected. This demonstrated that binding of ATP and ADP can be

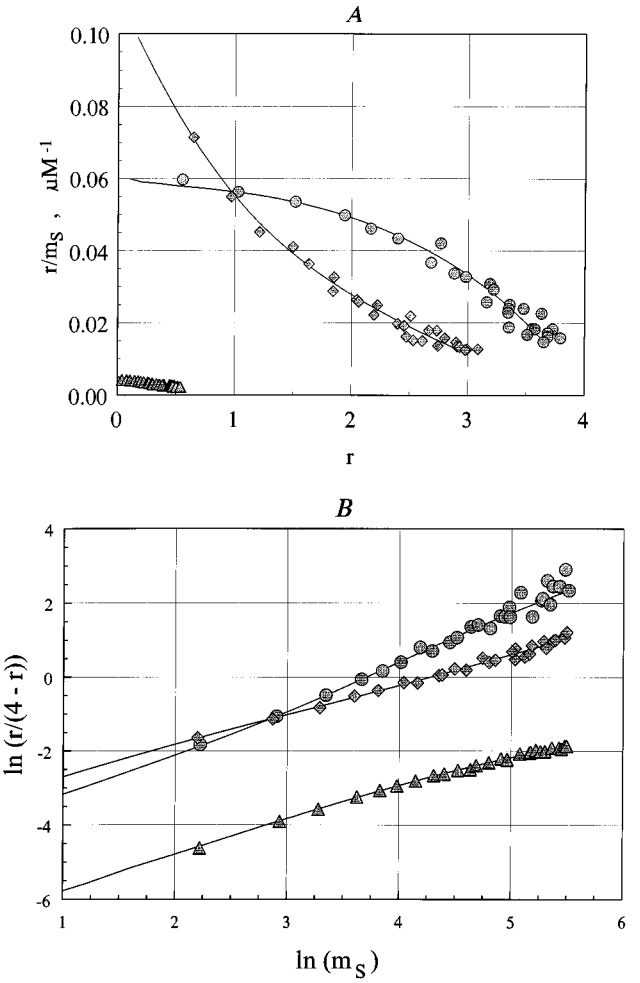

FIGURE 4: Scatchard and Hill plots for the systems in Figure 3. (A) Scatchard plot: (Circle) ATP, concave to the *r*-axis; (square) ADP, convex to the *r*-axis; (triangle) AMP. (B) Hill plot: the isotherm is expressed in terms *r* rather than in terms of the classical fractional saturation; m_S is given in μM.

distinguished with our technique by using short incubation times with the hydrolyzable nucleotide.

No appreciable binding of MgAMP was observed. AMP-PNP produced binding plots that leveled off slightly lower than the ATP isotherms.

In Figure 4A, typical data are presented in the form of a Scatchard plot. The curves for both ATP and ADP deviate from linearity, with data for ATP being concave toward the *r*-axis and data for ADP being convex. This curvature suggests the existence of more than one distinct class of nucleotide binding site, with possible cooperative interactions. While it is reasonable to treat the convex curve for ADP in terms of independent sites, the concave curve for ATP binding is most simply interpreted in terms of cooperativity (see Discussion).

The Hill plots of the same data as Figure 4A are shown in Figure 4B. The plot of ATP gives a steeper slope at half-saturation than that of ADP. From the slopes, Hill coefficients of 1.4 and 0.8 are found for these two nucleotides in this dataset. A Hill coefficient greater than one can indicate positive cooperativity, less than one negative cooperativity, and equal to one noninteracting sites. The observed values that deviate from unity suggest that ATP and ADP binding may be cooperative; however, the extent of this hypothetical cooperativity is clearly low or moderate.

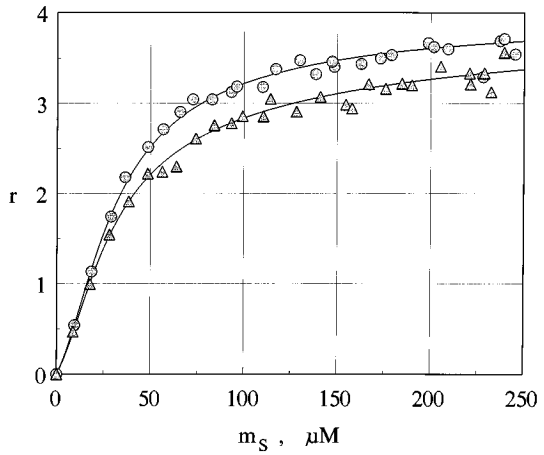

FIGURE 5: Effect of vanadate on MgATP and MgADP binding to the β heavy chain subunit of dynein. The binding isotherm was measured as described in the legend to Figure 1. in the presence of 50 μM vanadate. (Circle) MgATP; (triangle) MgADP. The difference between ATP and ADP is greatly diminished here as compared to Figure 3. The β chain concentration in the dextran phase was 4 μM.

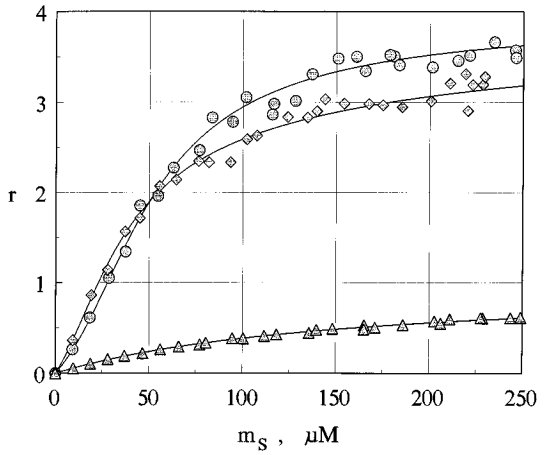

FIGURE 6: Effect of different cations on MgATP binding to the β heavy chain subunit of dynein. The conditions were the same as in Figure 1, except that Mg^{2+} was omitted and 0.5 mM Fe(III)-gluconate (circle), 1 mM Ca^{2+} (square), or 1 mM EDTA (triangle) was present. The β heavy chain concentration in the dextran phase was 4 μM.

Effect of Vanadate on Nucleotide Binding. The vanadate ion is a potent inhibitor of dynein ATPase that forms a dynein·ADP·vanadate ternary complex (Johnson, 1983). In the presence of 50 μM vanadate, MgATP and MgADP bind with similar affinity, with association constants close to those of ATP in the absence of vanadate (Figure 5). Thus the binding of the ADP/vanadate complex appears to resemble the binding of ATP more closely than that of ADP.

Effect of Divalent Cations on ATP Binding. The effects of various cations on the binding of ATP to the β heavy chain subunit are shown in Figure 6; similar results were obtained with the intact dynein. Iron (III)-gluconate (0.5 mM), which has been thought to bind at the Mg^{2+} binding site in the dynein/ATP complex (Mocz & Gibbons, 1990), supports binding of ATP with properties similar to Mg^{2+}. However, 1 mM Ca^{2+} supports binding of ATP with somewhat lower levels than Mg^{2+}, even when assayed in a 100 mM acetate medium in order to exclude possible complexation of Ca^{2+} with sulfate (Sillen & Martell, 1971). The differences in the ATP binding level with Ca^{2+} and Fe^{3+}

Table 1: Stepwise Equilibrium and Site-Binding Constants for Nucleotide Binding to Dynein[a]

stepwise site binding	K_1 k_1	K_2 k_2	K_3 k_3	K_4 k_4	
dynein/MgATP	3.3 ± 0.4	2.0 ± 0.2	1.7 ± 0.2	1.3 ± 0.2	(25)
	0.8	1.4	2.5	5.4	
β chain/MgATP	2.8 ± 0.4	3.0 ± 0.6	3.3 ± 0.5	1.7 ± 0.4	(8)
	0.3	1.0	2.0	5.0	
α chain/MgATP	0.8 ± 0.1	1.5 ± 0.2	1.8 ± 0.4	1.3 ± 0.4	(6)
	0.2	1.0	2.7	5.2	
dynein/MgADP	10.9 ± 0.3	2.1 ± 0.2	0.9 ± 0.3	0.2 ± 0.1	(12)
	2.7	1.4	1.3	0.9	
β chain/MgADP	6.7 ± 0.1	1.9 ± 0.2	5.7 ± 0.2	0.1 ± 0.1	(7)
	1.7	1.3	0.9	0.4	
tubulin/MgATP	0.4 ± 0.02				(12)

[a] All constants are given in units of $10^{-4} \times M^{-1}$. Numbers in parentheses indicate the number of individual datasets used for each substrate. Uncertainties shown are standard errors.

are apparently not related to the capability of these cations to support ATPase activity, as the level of Triton activated ATPase is ~40% with Ca^{2+} (Evans et al., 1986) and ~10% with Fe^{3+} compared to that obtainable with Mg^{2+} (Mocz & Gibbons, 1990).

No significant binding of ATP was observed in the apparent absence of divalent cations, i.e., in the presence of 0.5−1 mM EDTA. This requirement of metals for nucleotide binding is in agreement with the ATPase properties of dynein (Evans et al., 1986). Furthermore, it indicated that ATP does not bind in a nonspecific manner to dynein under the experimental conditions.

Multiple Stepwise Analysis. The binding isotherms obtained in this study are consistent with a 1:4 complex between dynein and nucleotides. Table 1 gives the stoichiometric binding constants, as calculated by fitting these isotherms to the primary data using the simplex procedure. Although we have no proof that the K_i values obtained correspond to a global minimum, the excellent fits, measured by an absolute error function, provide some justification for using these values as adequate estimates of the association constants. Use of the Levenberg−Marquardt nonlinear fitting algorithm gave a clearly less good visual fit but still provided K_i values that agreed in order of magnitude.

The calculated constants indicate that the four binding sites are not equivalent, for if they were identical the relative values of K_i would be in the proportions 4, 3/2, 2/3, and 1/4 (Connors, 1987), which is clearly not the case.

The calculated overall site-binding constants progressively increase for MgATP and decrease for MgADP (Table 1) confirming heterogeneity in the binding affinities of the nucleotide sites, such as may derive from distinct classes of sites on dynein. Furthermore, the nearly monotonic increase and decrease in the respective site-binding constants can be an indication of possible cooperativity, which was also apparent in the Scatchard and Hill representation (Figure 4).

DISCUSSION

The results of this paper support a multiple nucleotide binding hypothesis for dynein. The stepwise binding model provides a good description of the binding isotherm that we have observed. MgATP nearly saturates all four sites at moderate concentrations of nucleotide, whereas MgADP saturates only three sites under comparable conditions and requires a much higher concentration of MgADP to saturate the fourth site. Although our data do not directly prove that all four nucleotide-binding sites reside on the dynein heavy chains rather than on one of the associated smaller subunits, the fact that preparations of the separated α and β heavy chain subfractions bind nucleotide to the same molar extent as intact dynein makes it likely that the observed binding sites all reside on the heavy chains.

The interaction of nucleotides with dynein appears to be largely a function of the phosphate group. Increasing the phosphorylation of nucleotides produces a corresponding increase in the affinity of dynein for these compounds, with little or no affinity for AMP and micromolar to submillimolar affinity levels for ATP. The different affinities of ADP and ATP suggest that addition of phosphate contributes significantly to the overall affinity and may indicate the presence of major structural or chemical changes during formation of the ATP complex. The results also show the requirement of divalent cations for tight nucleotide binding. Neither ATP nor ADP binds in the absence of Mg^{2+}.

The binding constants determined from this analysis are likely to represent a useful approximation to the actual equilibrium constants for dynein under physiological conditions. Our values for the first two dissociation constants ($1/K_i$) for ATP binding are ~30 and 50 μM, respectively, and ~10 and 50 μM for ADP. These are reasonably close to the two ATPase K_m kinetic constants of 8−11 and 66−80 μM obtained for *Chlamydomonas* dynein (Wilkerson & Witman, 1995). The ~20% dextran in the lower phase of our phase system presumably has different dielectric properties and solvation characteristics than a physiological medium, and these might affect the nucleotide binding properties of dynein or the solvation properties of the nucleotides. Such might be the case with CaATP or CaADP which appeared to exhibit reduced binding affinities, presumably due to a difference in the hydration of Ca^{2+} relative to Mg^{2+}. Taken together, these considerations suggest that the values for K_i obtained here may be somewhat lower than physiological ones.

Nucleotide polyphosphates are present at micromolar to millimolar levels in the cell. Thus regulation of dynein activity may occur through the binding of such ligands. Given the physiological nucleotide concentrations in the sperm flagellum and the K_i values for nucleotide binding, it seems likely that all four binding sites on the chain are occupied by ATP or ADP to a significant extent *in vivo*. Since the values of K_3 and K_4 are not greatly different from K_2, such nucleotides bound at noncatalytic sites may not be replaced during several turnovers at the catalytic site of the dynein. Is it possible that the noncatalytic sites must be filled for ATP hydrolysis to occur under physiological conditions? If not, do the noncatalytic sites have an essential role in the hydrolysis step? Possible fluctuations of ATP and ADP concentrations could change the noncatalytic site nucleotide loading and produce useful modulations of ATP hydrolysis properties. Whether such effects operate mechanistically by affecting binding at the catalytic site or by direct modulation of dynein properties, remains to be determined.

Scatchard plots derived from the binding isotherms suggest that nucleotide binding to dynein may be a cooperative process. A convex Scatchard plot is obtained if the binding of a charged nucleotide ligand to multiple sites on dynein were to alter significantly the electrostatic potential at the dynein surface so that the successive binding of the nucle-

otide ligands became more difficult. This could also be a steric or entropic effect in which binding at all sites would require a highly regular arrangement of bound nucleotides which is entropically unfavorable. The opposite is true for a concave plot.

Representation of the binding data in the form of Hill plots can provide an indication of the extent of possible cooperativity. The observed Hill coefficients are well below the maximum number of sites obtained from the direct binding isotherms but clearly deviate from a coefficient unity. In agreement with the Scatchard representation, this may suggest low to moderate levels of cooperativity in which the sites do not act in a wholly all-or-none fashion.

To obtain insight into the mechanism responsible for this hypothetical cooperativity, it is not sufficient to compare the values of the stepwise binding constants. In this work distinction between a noncooperative model and negative and positive cooperativity was sought by evaluating the corresponding site-binding constants. In this context, ADP binding lead to situations where the site-binding constants progressively decreased in value indicating possible negative cooperativity, in agreement with the Scatchard and Hill type representation. ATP binding exhibited the opposite behavior suggesting the possibility that the dynein/MgATP systems are positively cooperative; that is, binding at the lower affinity sites decreases the dissociation rate of nucleotide from a higher affinity site. Positive cooperativity is a rare phenomenon and, in the case of dynein, might possibly be due to conformational changes in the molecule. Such a conformational change would permit a better charge interaction with ATP, but not with ADP. However, ADP and vanadate together appeared better able to imitate the charge distribution of ATP, as it was evidenced by their more similar binding isotherms. While general charge effects of bound nucleotide may play a role in the mechanism of negative cooperativity, the occurrence of positive cooperativity can only be discussed in general terms by postulating conformational changes in the dynein.

Evidence from proteolytic digestion supports the occurrence of a conformational change in dynein upon nucleotide binding and suggests that a broad region around the P1 loop is especially affected (Inaba et al., 1989; Mocz & Gibbons, 1991). This agrees with electron microscopic observations in which the morphology of dynein heads is distinctly different in the presence and absence of nucleotides (Goodenough & Heuser, 1985). Interactions between the α and β heavy chains have been shown to change with ATP (Inaba et al., 1990). Measurements of tryptophanyl fluorescence also indicate structural changes of dynein in conjunction with ATP binding (Mocz et al., 1991). Taken together, these observations strongly favor a cooperative nucleotide binding mechanism. The significance of such cooperativity in dynein function, however, requires additional evidence.

In conclusion, we note that the amino acid sequence motifs indicative of four nucleotide binding sites on dynein heavy chains have been well conserved in all axonemal and cytoplasmic dyneins studied to date. This conservation is indicative of their fulfilling substantive functions in the diverse forms of cell motility that result from the interaction of dynein with microtubules.

ACKNOWLEDGMENT

We thank Dr. Barbara H. Gibbons for helpful comments on the manuscript.

REFERENCES

Albertson, P. A. (1983) Interaction between biomolecules studied by phase partition, *Methods Biochem. Anal. 29*, 1−24.

Asai, D. J., & Lee, S. W. (1995) The structure and function of dynein heavy chains, *Mol. Cells 5*, 299−305.

Bell, C. W., & Gibbons, I. R. (1982) Structure of the dynein-1 outer arm in sea urchin sperm flagella. Analysis by proteolytic cleavage, *J. Biol. Chem. 257*, 516−522.

Bell, C. W., Fraser, C., Sale, W. S., Tang, W.-J. Y., & Gibbons, I. R. (1982) *Methods Cell Biol. 24*, 373−397.

Connors, K. A. (1987) *Binding Constants. The Measurement of Molecular Complex Stability*, pp 78−86, John Wiley & Sons, New York.

Cooper, J. W. (1981) Simplex optimization of variables, In *Introduction to Pascal for Scientists*, pp 185−197, John Wiley and Sons, New York.

Curthoys, N. P., & Rabinowitz, J. C. (1971) Formyltetrahydropholate synthetase. Binding of adenosine triphosphate and related ligands determined by partition equilibrium, *J. Biol. Chem. 246*, 6942−6952.

Evans, A., & Gibbons, I. R. (1986) Activation of dynein 1 adenosine triphosphatase by organic solvents and by Triton X-100, *J. Biol. Chem. 261*, 14044−14048.

Evans, J. A., Mocz, G., & Gibbons, I. R. (1986) Activation of dynein 1 adenosine triphosphatase by monovalent salt and inhibition by vanadate, *J. Biol. Chem. 261*, 14039−14043.

Fletcher, J. E., Spector, A. A., & Ashbrook, J. D. (1970) Analysis of macromolecule-ligand binding by determination of stepwise equilibrium constants, *Biochemistry 9*, 4580−4587.

Gibbons, B. H., Asai D. J., Tang, W, J.-Y, Hays, T. S., & Gibbons, I. R. (1994) Phylogeny and expression of axonemal and cytolasmic dynein genes in sea urchin, *Mol. Biol. Cell. 5*, 57−70.

Gibbons, I. R. (1963) Studies on the protein components of cilia from Tetrahymena pyriformis, *Proc. Natl. Acad. Sci. U.S.A. 50*, 1002−1010.

Gibbons, I. R. (1966) Studies on the adenosine triphosphatase activity of 14S and 20S dynein from cilia of Tetrahymena, *J. Biol. Chem. 241*, 5590−5596.

Gibbons, I. R. (1981) Cilia and flagella of eukaryotes. Discovery in cell biology, *J. Cell Biol. 91*, 107s−124s.

Gibbons, I. R. (1989) Microtubule-based motility, An overview of a fast-moving field. in Cell Movement: The Dynein ATPases (Warner, F. D., Satir, P., Gibbons, I. R., Eds.) Vol. 1, pp 3−22, Alan R Liss Inc., New York.

Gibbons, I. R, & Mocz, G. (1990) Vanadate sensitized photocleavage of proteins. in *Vanadium in Biological Systems* (Chasteen, N. D., Ed.) pp 143−142, Kluwer Academic Publishers, Dordrecht, The Netherlands.

Gibbons, I. R., Lee-Eiford, A., Mocz, G., Phillipson, C. A., Tang, W.-J. Y., & Gibbons, B. H. (1987) Photosensitized cleavage of dynein. heavy chains, cleavage at the "V1 site" by irradiation at 365 nm in the presence of ATP and vanadate, *J. Biol. Chem. 262*, 2780−2786.

Gibbons, I. R., Gibbons, B. H., Mocz, G., & Asai, D. J. (1991) Multiple nucleotide binding sites in the sequence of dynein β heavy chain, *Nature 352*, 640−643.

Gray, C. W., & Chamberlin, M. J. (1971) Measurement of ligand-protein binding interactions in a biphasic aqueous polymer system, *Anal. Biochem. 41*, 83−104.

Goodenough, U., & Heuser, J. (1985) Substructure of inner dynein arms, radial spokes and the central pair/projection complex of cilia and flagella, *J. Cell. Biol. 100*, 2008−2018.

Hays, T. S, Porter, M. E, McGrail, M., Grissom, P., Gosch, P., Fuller, M. T., & McIntosh, J. R. (1994) A cytoplasmic dynein motor in *Drosophila*, identification and localization during embryogenesis, *J. Cell. Sci. 107*, 1557−1569.

Inaba, K., & Mohri, H., (1989) Dynamic conformational changes of 21 S dynein ATPase coupled with ATP hydrolysis revealed by proteolytic digestion, *J. Biol. Chem. 264*, 8384−8388.

Inaba, K., Ono, M., & Mohri, H. (1990) Conformational changes of the β chain of the outer-arm dynein from sea urchin sperm flagella coupled with ATP hydrolysis, *J. Biochem. (Tokyo) 108*, 663−668.

Johnson, K. A. (1983) The pathway of ATP hydrolysis by dynein. Kinetics of a presteady state phosphate burst, *J. Biol. Chem. 258*, 13825−13832.

Kinoshita, S., Miki-Noumura, T., & Omoto, C. K. (1995) regulatory role of nucleotides in axonemal function, *Cell Motil. Cytoskel. 32*, 46−54.

Koonce, M. P, & McIntosh J. R. (1992) Dynein from *Dictyostelium*, Primary structure comparisons between a cytoplasmic motor enzyme and flagellar dynein, *J. Cell. Biol. 119*, 1597−1604.

LeBel, D., Poirier, G. G., & Beaudon, A. R. (1978) A convenient method for the ATPase assay, *Anal. Biochem. 85*, 86−89.

Li, Y. Y., Yeh, E., Hays, T., & Bloom, K. (1993) Disruption of a mitotic spindle mutant in a yeast dynein mutant, *Proc. Natl. Acad. Sci. U.S.A. 90*, 10096−10100.

Lye, R. J., Porter, M, E., Scholey, J. M., & McIntosh, J. R. (1987) Identification of a microtubule-based cytoplasmic motor in the nematode C. elegans, *Cell 51*, 309−318.

Mikami, A., Paschal, B. M., Mazumdar, M., & Vallee, R .B. (1993) Molecular cloning of the retrograde transport motor cytoplasmic dynein MAP 1C, *Neuron 10*, 787−796.

Mitchell, D. R., & Brown, K. S. (1994) Sequence analysis of the Chlamydomonas α and β dynein heavy chain genes, *J. Cell Sci. 107*, 635−644.

Mocz, G., & Gibbons, I. R. (1990) Iron(III)-mediated photolysis of outer dynein ATPase from sea urchin sperm flagella, *J. Biol. Chem. 265*, 2917−2922.

Mocz, G., & Gibbons, I. R. (1995) Partition analysis for measuring the equilibrium binding between nucleotides and axonemal dynein, *Mol. Biol. Cell. 6*, 33a.

Mocz, G, Farias, J., & Gibbons, I. R. (1991) Proteolytic analysis of domain structure in the β heavy chain from sea urchin sperm flagella, B*iochemistry 30*, 7225−7231.

Neely, M. D., Erickson, H. P., & Boekelheide, K. (1990) HMW-2, the Sertoli cell cytoplasmic dynein from rat testis, is a dimer composed of nearly identical subunits, *J. Biol. Chem. 265*, 8691−8698.

Nichol, L. W., & Winzor, D. J. (1981) Binding equations and control effects, In *Protein−Protein Interactions* (Frieden, C., Nichol, L. W., Eds.) p 337−380, John Wiley and Sons, New York.

O'Brien, E. T., & Erickson, H. P. (1989) Assembly of pure tubulin in the absence of free GTP, Effect of magnesium, glycerol, ATP, and the nonhydrolyzable GTP analogues, *Biochemistry 28*, 1413−1422.

Ogawa, K. (1991) Four ATP-binding sites in the midregion of the β heavy chain of dynein, *Nature 352*, 643−645.

Ogawa, K., & Mohri, I. (1972) Studies on flagellar ATPase from sea urchin spermatozoa I. Purification and some properties of the enzyme, *Biochim. Biophys. Acta 256*, 142−155.

Omoto, C. K., Yagi, T., Kurimoto, E., & Kamiya, R. (1996) Ability of paralyzed flagella mutants of Chlamydomonas to move, *Cell Motil. Cytoskel. 33*, 88−94.

Pallini, V., Bugnoli, M., Mencarelli, C., & Scapigliati, G. (1982) Biochemical properties of ciliary, flagellar and cytoplasmic dyneins, In *Prokaryotic and Eukaryotic Flagella*, pp 339−352, London, Cambridge University Press.

Pallini, V., Mencarelli, C., Bracci, L., Contorni, M., Ruggiero, P., Tiezzi, A., & Manetti, R. (1983) Cytoplasmic nucleoside-triphosphatases similar to axonemal dynein occur in widely different cell types, *J. Submicrosc. Cytol.* 15, 229−235.

Paschal, B. M, Shpetner, H. S , & Vallee, R. B. (1987) MAP1C is a microtubule-associated ATPase which translocates microtubules in vitro and has dynein-like properties, *J. Cell Biol. 105*, 1273−1282.

Press, W., H., Flannery, B. P., Teukolsky, S. A., & Vetterling, W. T. (1992) Nonlinear Models, in *Numerical Recipes in Pascal, The Art of Scientific Computing*, pp 572−580, Cambridge University Press, Cambridge.

Raghupathi, R. N., & Diwan, A. M. (1994) A protocol for protein estimation that gives a nearly constant color yield with simple proteins and nullifies the effect of four known interfering agents, Microestimation of peptide groups, *Anal. Biochem. 219*, 356−359.

Sale, W. S., & Fox, L. A. (1988) Isolated β-heavy chain subunit of dynein translocates microtubules *in vitro*, *J. Cell Biol. 107*, 1793−1797.

Schnapp, B. J., & Reese, T. S. (1989) Dynein is the motor for retrograde axonal transport of organelles, *Proc. Natl. Acad. Sci. U.S.A. 85*, 1109−1113.

Shimizu, T., Furusawa, K., Ohashi, S., Toyoshima, Y. Y., Okuno, M., Malik, F., & Vale, R. (1991) Nucleotide specificity of the enzymatic and motile activities of dynein, kinesin and heavy meromyosin, *J. Cell. Biol. 112*, 1189−1197.

Sillen, L. G., & Martell, A. E. (1971) in Stability constants of metal ion complexes. Special publication No. 25, pp 136 and 251, The Chemical Society, Burlington House, London.

Vale, R. D., Soll, D. R., & Gibbons, I. R. (1989) One-dimensional diffusion of microtubules bound to flagellar dynein, *Cell 59*, 915−925.

Vallee, R. B., Wall, J. S., & Paschal, B. M. (1989) The role of dynein in retrograde axonemal transport, *Trends Neurosci. 12*, 66−70.

Walker, J. A., Saraste, M., Runswick, M. J., & Gay, N. K. (1982) Distinctly related sequences in the α and β-subunits of ATP synthase, myosin, kinases and other ATP-requiring enzymes and a common nucleotide binding fold, *EMBO J. 1*, 945−951.

Whitaker, J. R., & Granum, P. E. (1980) An absolute method for protein determination based on difference in absorbance at 235 and 280 nm, *Anal. Biochem. 109*, 151−159.

Wilkerson, C. G., & Witman, G. B. (1995) Dynein heavy chains have at least two functional ATP-binding sites, *Mol. Biol. Cell 6*, 33a.

Wilkerson, C. G., King, S. M., & Witman, G. B. (1994) Molecular analysis of the γ heavy chain of Chlamydomonas flagellar outer-arm dynein, *J. Cell Sci. 107*, 497−506.

BI960662U